

Characterization of XIAP-Deficient Mice

HELENA HARLIN,¹ STEPHANIE BIRKEY REFFEY,² COLIN S. DUCKETT,² TULLIA LINDSTEN,³
AND CRAIG B. THOMPSON^{1,3*}

Committee on Immunology, Department of Medicine, University of Chicago, Chicago, Illinois 60637¹; Metabolism Branch, Division of Clinical Sciences, National Cancer Institute, National Institutes of Health, Bethesda, Maryland 20892²; and Departments of Cancer Biology and Pathology and Laboratory Medicine, Abramson Family Cancer Research Institute, University of Pennsylvania, Philadelphia, Pennsylvania 19104³

Received 11 December 2000/Returned for modification 20 December 2000/Accepted 15 February 2001

The inhibitor of apoptosis protein (IAP) family consists of a number of evolutionarily conserved proteins that function to inhibit programmed cell death. X-linked IAP (XIAP) was cloned due to its sequence homology with other family members and has previously been shown to prevent apoptosis by binding to active caspases 3, 7, and 9 in vitro. XIAP transcripts can be found in a variety of tissues, and the protein levels are regulated both transcriptionally and posttranscriptionally. To better understand the function of XIAP in normal cells, we generated mice deficient in XIAP through homologous gene targeting. The resulting mice were viable, and histopathological analysis did not reveal any differences between XIAP-deficient and wild-type mice. We were unable to detect any defects in induction of caspase-dependent or -independent apoptosis in cells from the gene-targeted mice. One change was observed in cells derived from XIAP-deficient mice: the levels of c-IAP1 and c-IAP2 protein were increased. This suggests that there exists a compensatory mechanism that leads to upregulation of other family members when XIAP expression is lost. The changes in c-IAP1 and c-IAP2 expression may provide functional compensation for loss of XIAP during development or in the induction of apoptosis.

Viruses, in order to propagate more efficiently, have evolved several strategies to prevent infected cells from dying. One common mechanism utilized by viruses is to block the host cell's apoptotic machinery, and viral genomes thus often encode proteins that have antiapoptotic properties. The X-linked inhibitor of apoptosis protein (XIAP), also known as IAP-like protein or mammalian IAP homologue A, was originally cloned as a mammalian homologue of the IAP family of viral proteins. The IAPs are expressed in baculoviruses and function to prevent the programmed cell death of infected cells. XIAP is ubiquitously expressed in all normal tissues (6, 7, 16).

XIAP contains two types of conserved sequence motifs, the baculovirus IAP repeats (BIRs) and the zinc finger-like RING finger. The BIRs are located at the amino-terminal end of the protein, and XIAP contains three repeats, whereas two repeats are found in the viral proteins. The nuclear magnetic resonance structures of BIRs 2 and 3 have recently been described (22, 23). The two BIRs have similar characteristics and resemble a classical zinc finger. The RING finger, believed to mediate protein-protein interactions, is situated at the carboxyl terminus of the protein.

Cells transfected with XIAP are able to block programmed cell death in response to a variety of apoptotic stimuli (5, 6, 29). It has been shown that recombinant XIAP is able to specifically block the activity of caspases 3, 7, and 9 (2, 4). In human cells, XIAP can itself be cleaved by caspases (3) and cleavage of endogenous XIAP can be detected in T lymphocytes undergoing apoptosis (13). The two cleaved fragments

are still able to inhibit caspase activity (3). The cleavage occurs in the spacer region between BIR 2 and BIR 3 and correlates with the caspase-binding specificity of XIAP; the second BIR associates with caspases 3 and 7 (22, 24) while the third BIR binds caspase 9 (23).

Two closely related family members with the same overall structure as XIAP, c-IAP1 and c-IAP2, have been identified (16, 17, 27). These proteins were cloned due to their association with tumor necrosis factor (TNF) receptor-associated factors (TRAFs) 1 and 2 (17). The interaction of the TRAFs with the c-IAPs does not involve the RING finger domain of either the c-IAPs or the TRAFs, but instead, the BIRs bind to the TRAF domain. Although XIAP has not been shown to associate with any TRAF family members, the c-IAPs may have other functions in common with XIAP. They all share the ability to specifically inhibit active caspases 3 and 7 (4, 18), but only XIAP is able to block caspase 9. This difference in specificity for caspase 9 correlates with structural differences in the third BIR between XIAP and c-IAP1 (11, 23). Four more distantly related mammalian family members, NAIP (19), Survivin, (1) BRUCE (9), and Livin/ML-IAP1 (15, 28), have been identified in humans. All IAP-like proteins identified have been shown to have antiapoptotic properties in different systems. In addition, IAP family members have been identified in *Drosophila melanogaster* (10), *Caenorhabditis elegans* (8), and yeast (26), demonstrating an evolutionarily conserved role for these proteins.

Recently, some insights into the function of XIAP have been made. Firstly, XIAP was shown to interact with transforming growth factor β (TGF- β)-activated kinase 1 binding protein 1 (TAB1) in a *Xenopus* system for studying the bone morphogenic protein (BMP) signaling pathway (30). BMPs are members of the TGF- β family, and signaling by BMP2 or BMP4

* Corresponding author. Mailing address: Abramson Family Cancer Research Institute, Room 450, BRB II/III, 421 Curie Blvd., Philadelphia, PA 19104-6160. Phone: (215) 746-5515. Fax: (215) 746-5511. E-mail: craig@mail.med.upenn.edu.

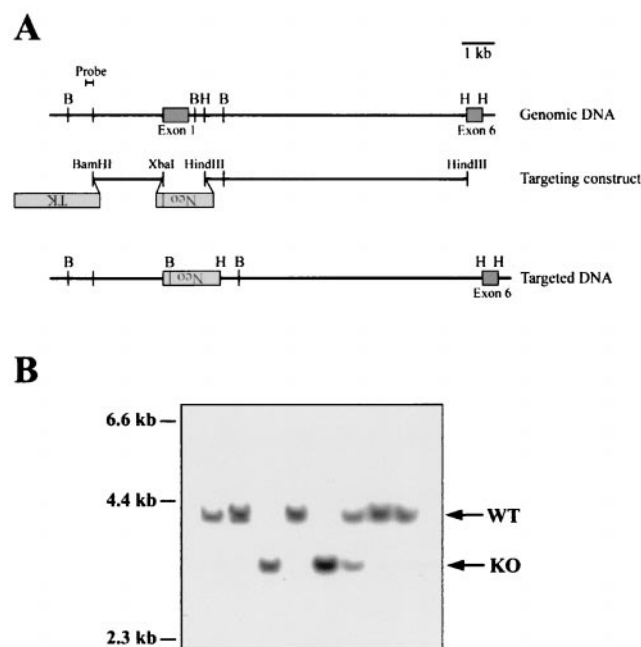


FIG. 1. Generation of XIAP-deficient mice by gene targeting. (A) Schematic representation of the targeting strategy used to disrupt the XIAP gene. The locations of exons 1 and 6 are shown. Exons 2 to 5 are contained within the 8.3-kb *HindIII-HindIII* fragment (not shown). The targeting construct replaces the coding sequence of exon 1 with the neomycin resistance gene, in the opposite transcriptional orientation. The sequence used as a probe to screen for homologously recombined DNA is shown. B (*BglII*) and H (*HindIII*) sites are shown for the genomic and targeted DNA. (B) Southern blot analysis of *BglII*-digested tail DNA from targeted mice. The WT allele is 4.0 kb, and the targeted allele is 3.2 kb. The blots were probed with the 0.2-kb *BamHI-EcoRI* fragment shown in panel A.

leads to downstream activation of TGF- β -activated kinase 1, a mitogen-activated protein kinase kinase that is activated by TAB1. The RING finger of XIAP is able to bind both to TAB1 and to an upstream BMP receptor (type 1), suggesting that XIAP may signal in a TGF- β -mediated pathway. Secondly, XIAP can be upregulated as a result of focal adhesion kinase overexpression (21). Focal adhesion kinase mediates signals from integrins and neuropeptides. Finally, levels of cellular XIAP protein appear to be carefully regulated at the posttranscriptional level. XIAP translation has been shown to be upregulated in response to physiological stress (12), and XIAP can be targeted for proteasome-dependent degradation upon proapoptotic stimuli (31).

XIAP has been shown to efficiently inhibit apoptosis in a number of in vitro systems. To further study the role of XIAP in vivo, mice deficient in the XIAP protein were generated by homologous gene targeting. Despite complete lack of XIAP expression, the XIAP-deficient mice were born at the expected Mendelian frequency, had no obvious physical or histological defects, and had normal life spans. No obvious defects in programmed cell death were seen after the induction of apoptosis using a variety of stimuli.

MATERIALS AND METHODS

Targeting strategy. A 0.7-kb *PstI-NcoI* fragment containing the first two BIRs of human *xiap* was used to screen a phage library (λ FIX II; Stratagene

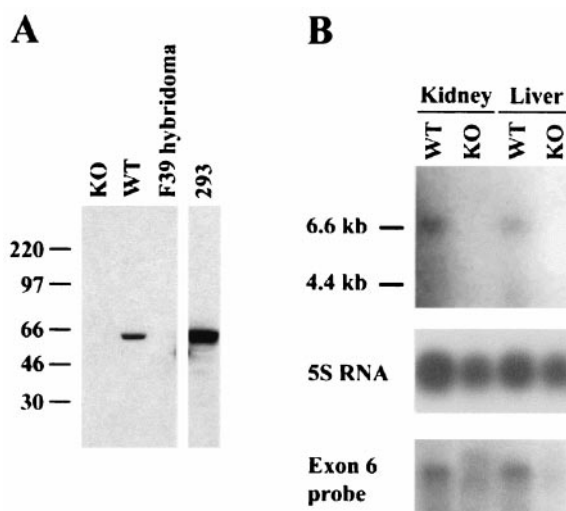


FIG. 2. Targeted mice have no detectable XIAP protein or mRNA. (A) Western blot analysis of lysate from WT or XIAP-deficient (KO) embryonic fibroblasts. Lysate from a hybridoma lacking XIAP expression (F39) was used as a negative control. Lysate from 293 cells served as a positive control. Molecular mass standards, in kilodaltons, are indicated on the left. (B) Northern blot analysis of RNA from WT or XIAP-deficient (KO) tissues. The top blot was probed with a fragment from exon 1, which is deleted in the KO tissues. The bottom blot shows a duplicate blot probed with a fragment from exon 6, which is not affected by XIAP gene targeting. The loading of RNA was verified using 5S rRNA.

Cloning Systems, La Jolla, Calif.) derived from 129/SvJ mice. The resulting genomic clones were mapped by restriction digest analysis, Southern blotting, and sequencing. The genomic organization of mouse *xiap* has also been published (7). A 2.2-kb *BamHI-XbaI* fragment located 5' of exon 1 and an 8.3-kb *HindIII-HindIII* fragment containing exons 2 to 6 were cut out from the same phage preparation and subcloned into the pPNT vector (25). Upon linearization, the resulting targeting construct contained the phosphoglycerate kinase (PGK)-*neo^r* cassette in a transcriptional orientation opposite that of the XIAP gene, in between the two subcloned genomic fragments that were flanked on one side by the PGK-thymidine kinase (TK) cassette.

Generation of XIAP-deficient mice. The electroporation, culture, and selection of *neo^r*, TK-negative embryonic stem (ES) cells were as previously described (20). The resulting expanded ES cell clones were screened by Southern blot analysis of *BglII*-digested genomic DNA isolated from each clone. The 0.2-kb *BamHI-EcoRI* probe used to identify homologously recombined ES cell clones is shown in Fig. 1A.

ES cells from three independent clones were injected into C57BL/6 blastocysts, and chimeric mice with a large contribution of targeted ES cells were identified due to their mainly agouti coat color. Largely agouti chimeras were bred to C57BL/6 females, and the resulting F₁ progeny were screened by Southern blot analysis of tail DNA to determine their genotype. Mice with germ line transmission of a targeted XIAP allele were intercrossed to generate XIAP-deficient mice.

Western and Northern blot analysis. Protein lysates were made as previously described (5). For the TNF-treated samples, confluent mouse embryonic fibroblasts were treated with 200 U of human TNF- α (Boehringer-Mannheim, Indianapolis, Ind.)/ml for 4 h at 37°C before the cells were lysed. Protein concentrations were determined by Bradford assay (Bio-Rad Laboratories, Hercules, Calif.). Protein samples (20 μ g [see Fig. 2] or 5 μ g [see Fig. 4]) were resolved by sodium dodecyl sulfate 4 to 12% gradient gel electrophoresis and then transferred to nitrocellulose membranes by electrophoretic blotting (Novex; Invitrogen, Carlsbad, Calif.). XIAP protein was detected using a monoclonal antibody raised against a protein fragment spanning human XIAP amino acids 268 to 426, containing the third BIR and the spacer region before the RING finger (catalog no. H59520; Transduction Laboratories, Lexington, Ky.). c-IAP1 protein was detected using a monoclonal antibody from the F39 hybridoma, which was raised against a fragment of c-IAP1 lacking the first BIR and which specifically recognizes c-IAP1. c-IAP2 protein was detected using a polyclonal antibody raised

TABLE 1. Lack of obvious phenotypic abnormalities associated with XIAP deficiency^a

Cell type	Stimulation	Readout
LN cell	α -CD3 plus or minus α -CD28	[³ H]thymidine incorporation
Draining LN cell	KLH immunization and in vitro restimulation	[³ H]thymidine incorporation, IL-2 and IL-4 production
Whole mouse	Response to infection with <i>Listeria monocytogenes</i>	CFU in spleen and liver on day 5
	Response to infection with <i>Leishmania major</i> ; in vitro restimulation with <i>L. major</i> antigen	Footpad swelling over time; [³ H]thymidine incorporation and IFN- γ production
Splenocyte and thymocyte	UV irradiation	% Apoptosis by PI exclusion
	Gamma irradiation	% Apoptosis by PI exclusion
CD4 ⁺ CD8 ⁺ thymocyte	α -CD3 injected i.p.	% Apoptosis by PI exclusion
Thymocyte	UV, PMA plus ionomycin	JNK activation
Mouse embryonic fibroblast	UV, anisomycin, TNF, heat shock, PMA plus ionomycin	JNK activation

^a Various assays in which XIAP-deficient mice or cells from these mice responded in a fashion similar to WT littermate controls are listed. Abbreviations: LN, lymph node; KLH, keyhole limpet hemocyanin; IL, interleukin; IFN- γ , gamma interferon; i.p., intraperitoneally; PMA, phorbol myristate acetate; JNK, c-Jun N-terminal kinase.

against a peptide containing amino acids 507 to 524 of human c-IAP2 (R&D Systems Inc., Minneapolis, Minn.). Relative amounts of protein were visualized using an antibody directed against β -tubulin (BD Pharmingen, San Diego, Calif.). Antibody detection was performed using an enhanced chemiluminescence detection system (Amersham-Pharmacia, Piscataway, N.J.).

Total RNA was purified from wild-type (WT) and knockout (KO) mice using TRIzol (Gibco BRL, Grand Island, N.Y.). The RNA was equalized as previously described (14), and the concentration was later determined by spectrophotometric analysis. Approximately 5 μ g of total RNA was used for each sample. The samples were loaded on an agarose gel, electrophoresed, and blotted as previously described (14). XIAP transcripts were detected using either a 0.8-kb *Xba*I-*Nco*I probe containing exon 1 or a 0.5-kb *Hind*III-*Hind*III probe containing the RING domain (exon 6). The relative amounts of RNA were visualized using an end-labeled 5S RNA probe.

Induction of cell death. (i) Fas-mediated apoptosis. Single cell suspensions from the thymus of WT or XIAP-deficient mice were plated on 24-well plates at 10⁶ cells/well. Anti-Fas antibody (Jo2) or isotype control antibody (BD Pharmingen) was added to a final concentration of 1 μ g/ml. Apoptotic CD4⁺ CD8⁺ cells were identified by staining the cells with fluorescein isothiocyanate-coupled anti-CD4 and phycoerythrin-coupled anti-CD8 antibodies (BD Pharmingen) in addition to propidium iodide (PI). The fluorescence-activated cell sorter (FACS) profiles were gated on CD4⁺ CD8⁺ cells, and the percentage of PI⁺ cells was determined.

(ii) UV irradiation and oligomycin-induced apoptosis. Mouse embryonic fibroblasts were generated from WT or XIAP-deficient embryos. Fifteen-day-old embryos were dissected away from surrounding extraembryonic membranes. Heads, tails, limbs, hearts, and livers were removed. Each embryo was cut into small pieces and incubated with rotation in 0.05% trypsin-EDTA (3 ml/embryo) (Gibco BRL) overnight at 4°C. The embryos were placed at 37°C for 30 min, broken up by pipetting, and then left to sediment for a few minutes. Cells still in suspension were collected, and sedimented material was treated twice more with fresh trypsin-EDTA solution for 30 min at 37°C, with cells in suspension collected after each incubation. The pooled cells were plated on tissue culture dishes and fibroblasts were allowed to grow out in Dulbecco's minimal essential medium (21).

Plated fibroblasts of equal degrees of confluency were UV irradiated for 30 s at 254 nm using a UV Stratalinker 2400 (Stratagene) (corresponding to 1,200 J m⁻²) or treated with 50 μ g of oligomycin (Sigma, St. Louis, Mo.)/ml. After 24 h, the percentage of apoptotic cells was determined by PI staining and FACS analysis.

RESULTS AND DISCUSSION

Gene targeting and generation of XIAP-deficient mice. The XIAP gene was disrupted by homologous gene targeting. Three independent ES cell lines were used to generate XIAP-deficient mice, using the targeting construct shown in Fig. 1A. This targeting strategy was chosen because it results in the deletion of exon 1, which is the largest of the six coding exons and contains the first two BIRs and half of the third. Thus, even if a partial transcript had been expressed in the targeted cells, the truncated protein would presumably not be functional. Figure 1B shows an example of Southern blot analysis of DNA from the offspring of breedings set up to generate XIAP-deficient mice. The probe used, shown in Fig. 1A, recognizes a 4.0-kb fragment from the WT allele and a 3.2-kb fragment from the targeted allele.

Mouse embryonic fibroblasts from mice that lack the WT allele had no detectable XIAP protein (Fig. 2A). The anti-XIAP antibody recognizes an epitope contained within the C-terminal part of the protein, and the DNA encoding this part was not deleted by the targeting construct, so the antibody should detect any residual XIAP protein. The Northern blot in Fig. 2B was hybridized with either a probe derived from exon 1 or a probe derived from exon 6, which is still present in the targeted allele. The XIAP-deficient RNA samples showed no distinct transcripts. We concluded that the targeting strategy used completely abolishes XIAP expression in the targeted mice.

XIAP-deficient mice were born at the expected Mendelian ratio, bred normally, and had no overt physical or behavioral abnormalities. Histological examination of selected tissues (heart, kidney, liver, lung, and brain) failed to show any differences between WT and XIAP KO mice (data not shown). The mice had life spans of greater than 1 year and did not

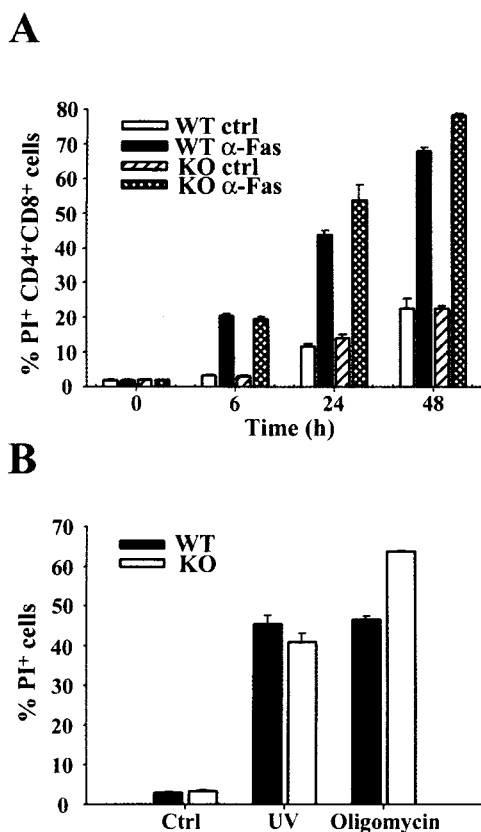


FIG. 3. Apoptosis occurs normally in XIAP-deficient mice. (A) Fas-mediated apoptosis of double-positive (CD4⁺ CD8⁺) thymocytes. WT or XIAP-deficient thymocytes were treated with either isotype control (ctrl) or anti-Fas (α-Fas) antibody. The percentage of apoptotic (PI⁺) cells was determined at the indicated time points. Cells from one WT and one KO mouse were plated in triplicate, and average values are shown along with the standard deviation for each triplicate sample. The data are representative of three separate experiments. (B) Caspase-dependent or -independent apoptosis. Embryonic fibroblasts were left untreated (ctrl) or treated with either UV irradiation or oligomycin. The percentage of apoptotic cells was determined at 24 h after treatment. WT and KO cells were plated in triplicate, and average values are shown along with the standard deviation for each triplicate sample. The data are representative of two separate experiments.

succumb to disease, even when kept in a non-barrier type animal facility. The mice had normal numbers of B cells as well as CD4⁺ and CD8⁺ T cells, as evidenced by FACS staining of thymus, spleen, and lymph node cells. In a variety of immunological assays, shown in Table 1, no significant differences could be observed between WT and XIAP-deficient mice. For these analyses and all others reported here, the XIAP KO mice were of a mixed genetic background between the 129S/SvJ and C57BL/6 strains. The WT mice used in each assay were littermates of the KO mice analyzed.

Induction of apoptosis occurs normally in XIAP-deficient mice. Since XIAP can act as an inhibitor of apoptosis in a variety of systems, we investigated whether programmed cell death was affected in the XIAP-deficient animals. Fas-mediated apoptosis occurs through direct activation of caspase 8, which in turn activates caspases 3 and 7, two of the caspases

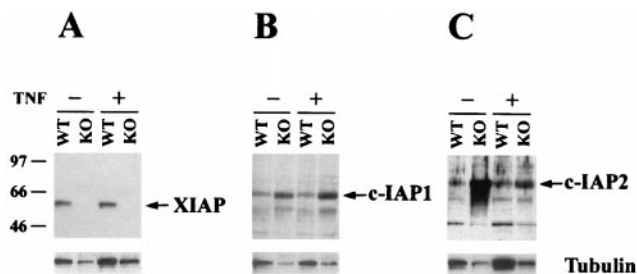


FIG. 4. Levels of c-IAP1 and c-IAP2 proteins are upregulated in XIAP-deficient cells. Western blot analysis of lysate from WT or XIAP-deficient (KO) embryonic fibroblasts. The cells were either untreated or stimulated with 200 U of human TNF-α/ml for 4 h. Gels were loaded in parallel, and the resulting blots were probed with antibodies directed against XIAP (A), c-IAP1 (B), or c-IAP2 (C). The blots were stripped and reprobed with an antibody against β-tubulin, shown at the bottom of each panel. Molecular mass standards, in kilodaltons, are indicated on the left.

that XIAP has been shown to inhibit *in vitro*. Fas-mediated apoptosis of thymocytes was analyzed (Fig. 3A). Treatment with anti-Fas monoclonal antibody *in vitro* induced similar levels of apoptosis in both WT and XIAP KO CD4⁺ CD8⁺ thymocytes, indicating that Fas-mediated apoptosis was not affected by loss of XIAP in this system. Since the two reports of endogenous XIAP being cleaved by caspases used Jurkat T cells or T lymphocytes to study this phenomenon (3, 13), thymocytes should be a valid cell type for detecting any abnormal regulation of apoptosis in the XIAP-deficient cells.

We next investigated whether UV irradiation- and oligomycin-induced apoptosis was affected in XIAP-deficient cells. Caspase 9-deficient embryonic fibroblasts are resistant to UV irradiation-induced apoptosis, and thus activation of this caspase ought to be required for UV-mediated apoptosis in this cell type. Caspase 9 activity can be inhibited by XIAP *in vitro*, and XIAP protein is present in embryonic fibroblasts (Fig. 2A). In contrast, oligomycin induces cell death in a caspase-independent manner, and this type of death-inducing stimulus would presumably not be affected by loss of XIAP. Embryonic fibroblasts were untreated, UV irradiated, or treated with oligomycin. No differences in the ability to undergo apoptosis were observed between WT and XIAP-deficient cells following UV irradiation at 1,200 J m⁻² or treatment with 50 μg of oligomycin/ml (Fig. 3B). Similar results were obtained using various doses of UV irradiation and concentrations of oligomycin (data not shown).

To characterize the XIAP-deficient mice further, we performed a number of assays focusing on a potential role for XIAP in the immune system and in particular in response to apoptotic stimulation. In numerous assays, cells from these mice responded in a manner indistinguishable from WT cells to both pro- and antiapoptotic stimuli (Table 1).

Levels of c-IAP1 and c-IAP2 are increased in XIAP-deficient cells. Since several mammalian homologues have been identified, it is possible that other family members are able to compensate for the lack of XIAP. To address this issue, we investigated the levels of c-IAP1 and c-IAP2 protein found in WT or XIAP-deficient embryonic fibroblasts that were either untreated or treated with TNF-α for 4 h. The tubulin levels for each sample were also determined, as a control for protein

loading. We noticed a consistent increase of c-IAP1 and c-IAP2 levels in the XIAP-deficient cells compared to the WT cells (Fig. 4), but no concomitant increase in tubulin expression was noticed. The levels of XIAP and c-IAP1 were not affected by TNF treatment, whereas the level of c-IAP2 decreased upon treatment. This result suggests that one potential explanation for the lack of a phenotype in XIAP-deficient mice is due to compensation by other family members.

It is also possible that we have not found the situation in which XIAP is critically important in preventing apoptosis *in vivo*, either because it is the only IAP family member expressed or because XIAP can function in a manner distinct from other family members.

In conclusion, despite a seemingly important role for XIAP in the inhibition of apoptosis in a variety of *in vitro* systems, XIAP-deficient mice do not have any obvious defects in development or in the regulation of apoptosis.

ACKNOWLEDGMENTS

This work was supported in part by grants from the National Institutes of Health.

Andras Nagy, Reka Nagy, and Wanda Abramow-Newerly are gratefully acknowledged for providing the RI ES cell line. We thank Daniel R. Brown for technical assistance with the *Leishmania major* studies and Maria-Luisa Alegre for critical review of the manuscript.

REFERENCES

- Ambrosini, G., C. Adida, and D. C. Altieri. 1997. A novel anti-apoptosis gene, survivin, expressed in cancer and lymphoma. *Nat. Med.* **3**:917–921.
- Datta, R., E. Oki, K. Endo, V. Biedermann, J. Ren, and D. Kufe. 2000. XIAP regulates DNA damage-induced apoptosis downstream of caspase-9 cleavage. *J. Biol. Chem.* **275**:31733–31738.
- Deveraux, Q. L., E. Leo, H. R. Stennicke, K. Welsh, G. S. Salvesen, and J. C. Reed. 1999. Cleavage of human inhibitor of apoptosis protein XIAP results in fragments with distinct specificities for caspases. *EMBO J.* **18**:5242–5251.
- Deveraux, Q. L., R. Takahashi, G. S. Salvesen, and J. C. Reed. 1997. X-linked IAP is a direct inhibitor of cell-death proteases. *Nature* **388**:300–304.
- Duckett, C. S., F. Li, Y. Wang, K. J. Tomaselli, C. B. Thompson, and R. C. Armstrong. 1998. Human IAP-like protein regulates programmed cell death downstream of Bcl-x_l and cytochrome c. *Mol. Cell. Biol.* **18**:608–615.
- Duckett, C. S., V. E. Nava, R. W. Gedrich, R. J. Clem, J. L. Van Dongen, M. C. Gilfillan, H. Shiels, J. M. Hardwick, and C. B. Thompson. 1996. A conserved family of cellular genes related to the baculovirus iap gene and encoding apoptosis inhibitors. *EMBO J.* **15**:2685–2694.
- Farahani, R., W. G. Fong, R. G. Korneluk, and A. E. MacKenzie. 1997. Genomic organization and primary characterization of miap-3: the murine homologue of human X-linked IAP. *Genomics* **42**:514–518.
- Fraser, A. G., C. James, G. I. Evan, and M. O. Hengartner. 1999. *Caenorhabditis elegans* inhibitor of apoptosis protein (IAP) homologue BIR-1 plays a conserved role in cytokinesis. *Curr. Biol.* **9**:292–301.
- Hauser, H. P., M. Bardroff, G. Pyrowolakis, and S. Jentsch. 1998. A giant ubiquitin-conjugating enzyme related to IAP apoptosis inhibitors. *J. Cell Biol.* **141**:1415–1422.
- Hay, B. A., D. A. Wassarman, and G. M. Rubin. 1995. *Drosophila* homologs of baculovirus inhibitor of apoptosis proteins function to block cell death. *Cell* **83**:1253–1262.
- Hinds, M. G., R. S. Norton, D. L. Vaux, and C. L. Day. 1999. Solution structure of a baculoviral inhibitor of apoptosis (IAP) repeat. *Nat. Struct. Biol.* **6**:648–651.
- Holcik, M., C. Yeh, R. G. Korneluk, and T. Chow. 2000. Translational upregulation of X-linked inhibitor of apoptosis (XIAP) increases resistance to radiation induced cell death. *Oncogene* **19**:4174–4177.
- Johnson, D. E., B. R. Gastman, E. Wiczkowski, G. Q. Wang, A. Amoscato, S. M. Delach, and H. Rabinowich. 2000. Inhibitor of apoptosis protein hIAP undergoes caspase-mediated cleavage during T lymphocyte apoptosis. *Cancer Res.* **60**:1818–1823.
- June, C. H., J. A. Ledbetter, M. M. Gillespie, T. Lindsten, and C. B. Thompson. 1987. T-cell proliferation involving the CD28 pathway is associated with cyclosporine-resistant interleukin 2 gene expression. *Mol. Cell. Biol.* **7**:4472–4481.
- Kasof, G. M., and B. C. Gomes. 2001. Livin, a novel inhibitor of apoptosis protein family member. *J. Biol. Chem.* **276**:3238–3246.
- Liston, P., N. Roy, K. Tamai, C. Lefebvre, S. Baird, G. Cherton-Horvat, R. Farahani, M. McLean, J. E. Ikeda, A. MacKenzie, and R. G. Korneluk. 1996. Suppression of apoptosis in mammalian cells by NAIP and a related family of IAP genes. *Nature* **379**:349–353.
- Rothe, M., M. G. Pan, W. J. Henzel, T. M. Ayres, and D. V. Goeddel. 1995. The TNFR2-TRAF signaling complex contains two novel proteins related to baculoviral inhibitor of apoptosis proteins. *Cell* **83**:1243–1252.
- Roy, N., Q. L. Deveraux, R. Takahashi, G. S. Salvesen, and J. C. Reed. 1997. The c-IAP-1 and c-IAP-2 proteins are direct inhibitors of specific caspases. *EMBO J.* **16**:6914–6925.
- Roy, N., M. S. Mahadevan, M. McLean, G. Shutler, Z. Yaraghi, R. Farahani, S. Baird, A. Besner-Johnston, C. Lefebvre, X. Kang, et al. 1995. The gene for neuronal apoptosis inhibitory protein is partially deleted in individuals with spinal muscular atrophy. *Cell* **80**:167–178.
- Shiels, H., X. Li, P. T. Schumacker, E. Maltepe, P. A. Padrid, A. Sperling, C. B. Thompson, and T. Lindsten. 2000. TRAF4 deficiency leads to tracheal malformation with resulting alterations in air flow to the lungs. *Am. J. Pathol.* **157**:679–688.
- Sonoda, Y., Y. Matsumoto, M. Funakoshi, D. Yamamoto, S. K. Hanks, and T. Kasahara. 2000. Anti-apoptotic role of focal adhesion kinase (FAK). Induction of inhibitor-of-apoptosis proteins and apoptosis suppression by the overexpression of FAK in a human leukemic cell line, HL-60. *J. Biol. Chem.* **275**:16309–16315.
- Sun, C., M. Cai, A. H. Gunasekera, R. P. Meadows, H. Wang, J. Chen, H. Zhang, W. Wu, N. Xu, S. C. Ng, and S. W. Fesik. 1999. NMR structure and mutagenesis of the inhibitor-of-apoptosis protein XIAP. *Nature* **401**:818–822.
- Sun, C., M. Cai, R. P. Meadows, N. Xu, A. H. Gunasekera, J. Herrmann, J. C. Wu, and S. W. Fesik. 2000. NMR structure and mutagenesis of the third Bir domain of the inhibitor of apoptosis protein XIAP. *J. Biol. Chem.* **275**:33777–33781.
- Takahashi, R., Q. Deveraux, I. Tamm, K. Welsh, N. Assa-Munt, G. S. Salvesen, and J. C. Reed. 1998. A single BIR domain of XIAP sufficient for inhibiting caspases. *J. Biol. Chem.* **273**:7787–7790.
- Tybulewicz, V. L., C. E. Crawford, P. K. Jackson, R. T. Bronson, and R. C. Mulligan. 1991. Neonatal lethality and lymphopenia in mice with a homozygous disruption of the c-abl proto-oncogene. *Cell* **65**:1153–1163.
- Uren, A. G., T. Beilharz, M. J. O'Connell, S. J. Bugg, R. van Driel, D. L. Vaux, and T. Lithgow. 1999. Role for yeast inhibitor of apoptosis (IAP)-like proteins in cell division. *Proc. Natl. Acad. Sci. USA* **96**:10170–10175.
- Uren, A. G., M. Pakusch, C. J. Hawkins, K. L. Puls, and D. L. Vaux. 1996. Cloning and expression of apoptosis inhibitory protein homologs that function to inhibit apoptosis and/or bind tumor necrosis factor receptor-associated factors. *Proc. Natl. Acad. Sci. USA* **93**:4974–4978.
- Vucic, D., H. R. Stennicke, M. T. Pisabarro, G. S. Salvesen, and V. M. Dixit. 2000. ML-IAP, a novel inhibitor of apoptosis that is preferentially expressed in human melanomas. *Curr. Biol.* **10**:1359–1366.
- Xu, D., Y. Bureau, D. C. McIntyre, D. W. Nicholson, P. Liston, Y. Zhu, W. G. Fong, S. J. Crocker, R. G. Korneluk, and G. S. Robertson. 1999. Attenuation of ischemia-induced cellular and behavioral deficits by X chromosome-linked inhibitor of apoptosis protein overexpression in the rat hippocampus. *J. Neurosci.* **19**:5026–5033.
- Yamaguchi, K., S. Nagai, J. Ninomiya-Tsuji, M. Nishita, K. Tamai, K. Irie, N. Ueno, E. Nishida, H. Shibuya, and K. Matsumoto. 1999. XIAP, a cellular member of the inhibitor of apoptosis protein family, links the receptors to TAB1-TAK1 in the BMP signaling pathway. *EMBO J.* **18**:179–187.
- Yang, Y., S. Fang, J. P. Jensen, A. M. Weissman, and J. D. Ashwell. 2000. Ubiquitin protein ligase activity of IAPs and their degradation in proteasomes in response to apoptotic stimuli. *Science* **288**:874–877.